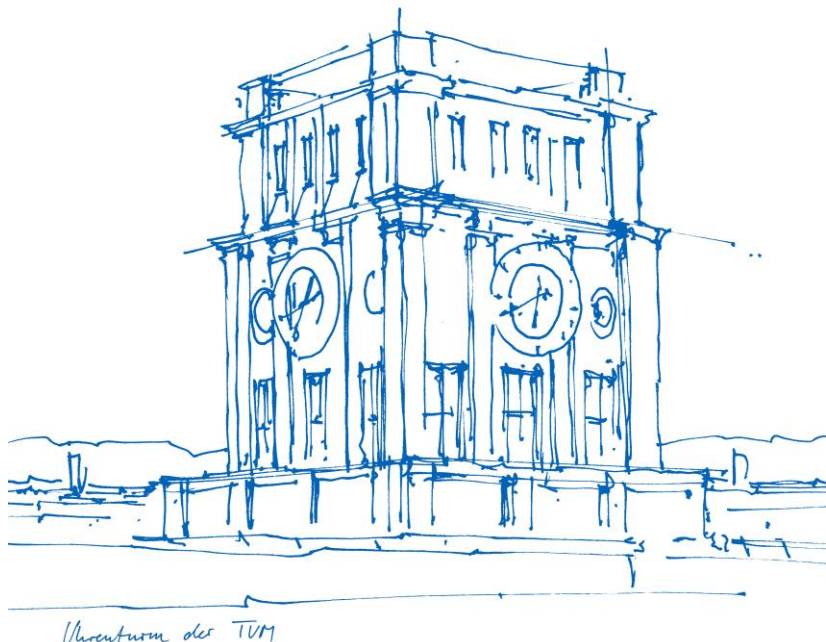


Energy transition in miniature: Combining catalysis and reaction engineering at a particle level

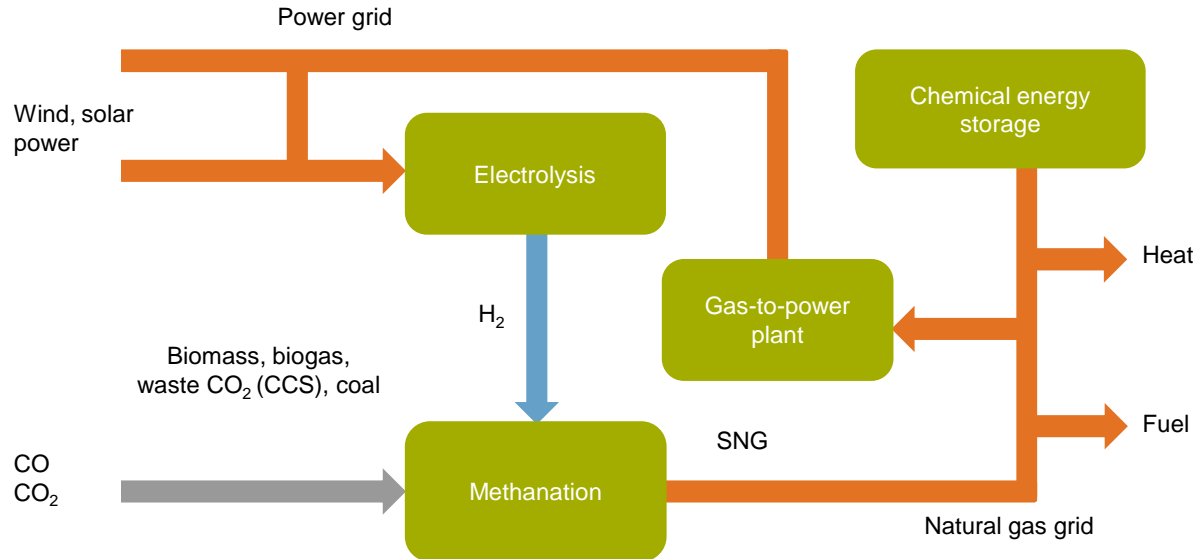
Olaf Hinrichsen
Catalysis Research Center
Technische Universität München



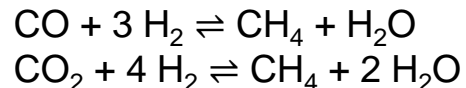
An aerial photograph of the Technical University of Munich (TUM) at Garching. The campus is a large, modern complex of white buildings with many glass windows, situated in a green, open landscape. A river flows through the area to the left of the campus. In the background, the city of Munich and the majestic Alps are visible under a clear blue sky.

Welcome to TUM@Garching!

Power-to-Gas (PtG) Concept



CO methanation
CO₂ methanation

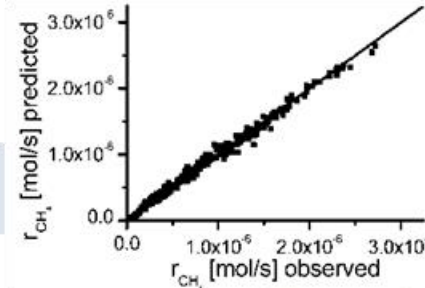


$$\Delta_R H^\circ = -206 \text{ kJ mol}^{-1}, \Delta_R G^\circ = -142 \text{ kJ mol}^{-1}$$
$$\Delta_R H^\circ = -165 \text{ kJ mol}^{-1}, \Delta_R G^\circ = -114 \text{ kJ mol}^{-1}$$

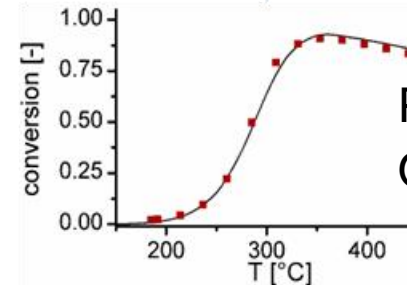
Kinetic measurements



Catalyst synthesis

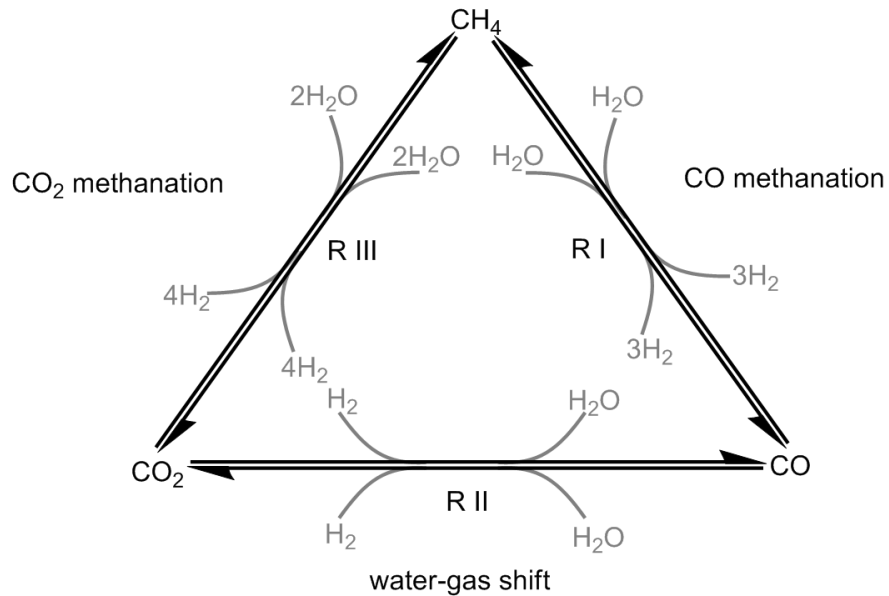
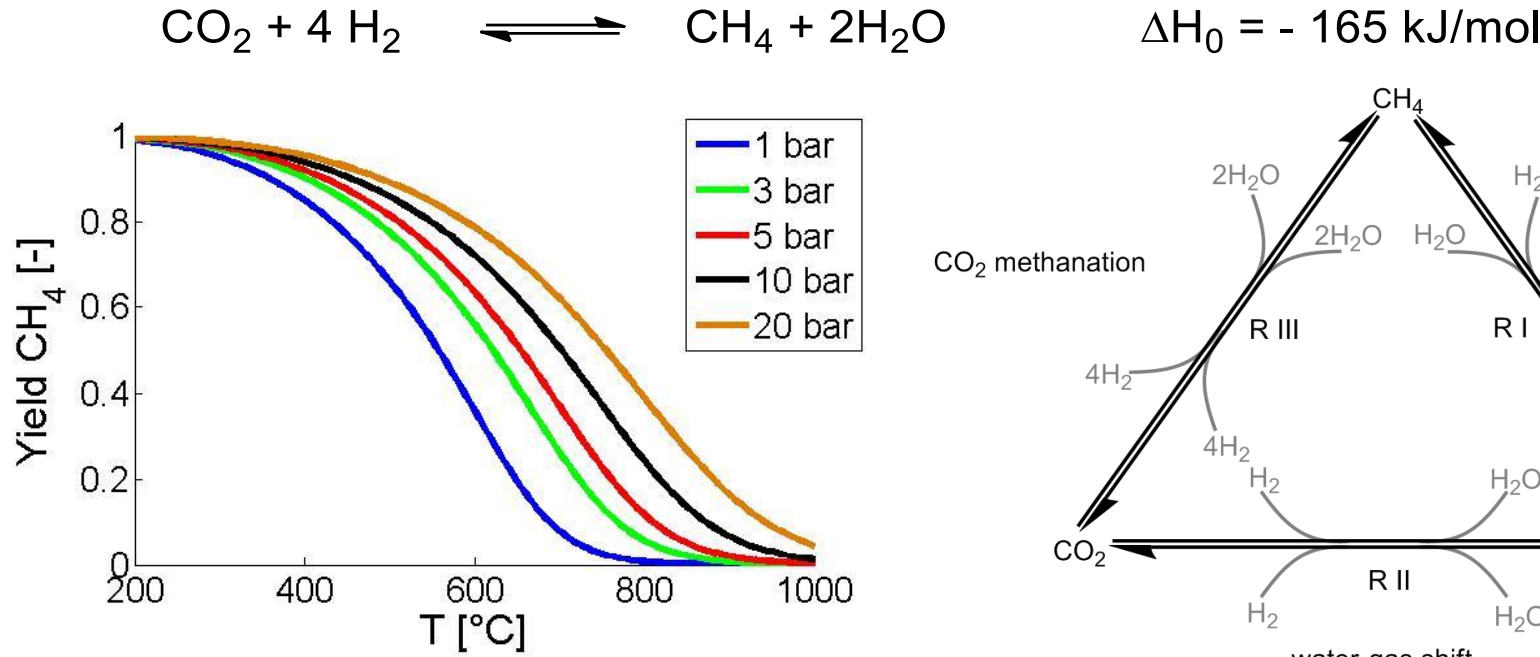


Modeling



Prediction & Optimization

Thermodynamics of the CO_2 Methanation Reaction

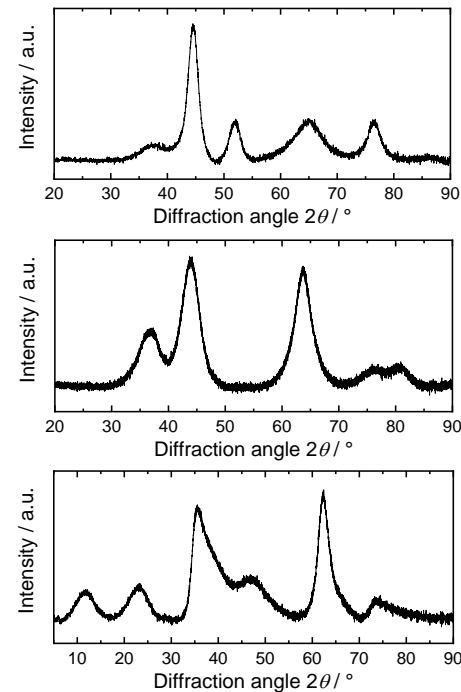
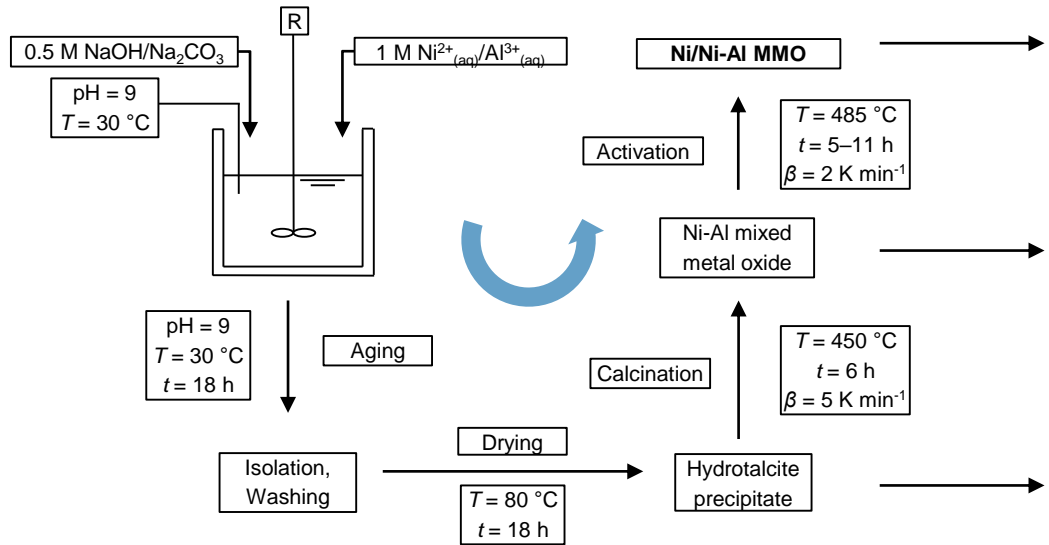


J. Xu, G.F. Froment, *AIChE J.* **1989**, *35*, 88–96.

D. Schlereth, O. Hinrichsen, *Chem. Eng. Res. Des.* **2014**, *92*, 702–712.

Catalyst Synthesis: Ni-Al mixed metal oxide catalysts

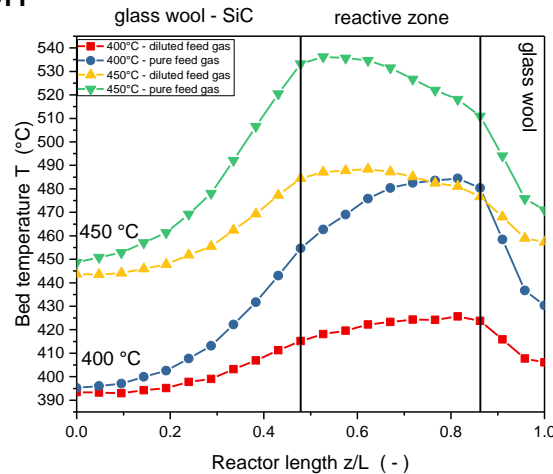
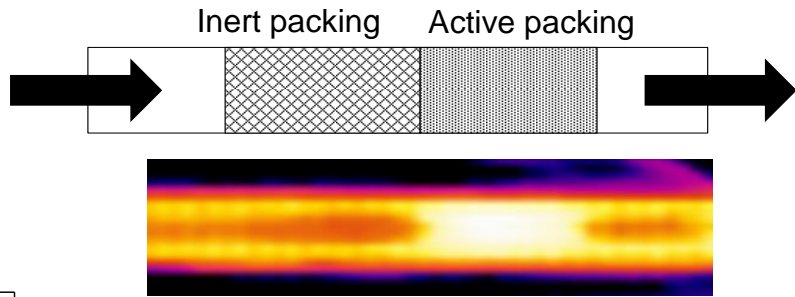
State-of-the-art / base catalyst: Ni-Al mixed metal oxide



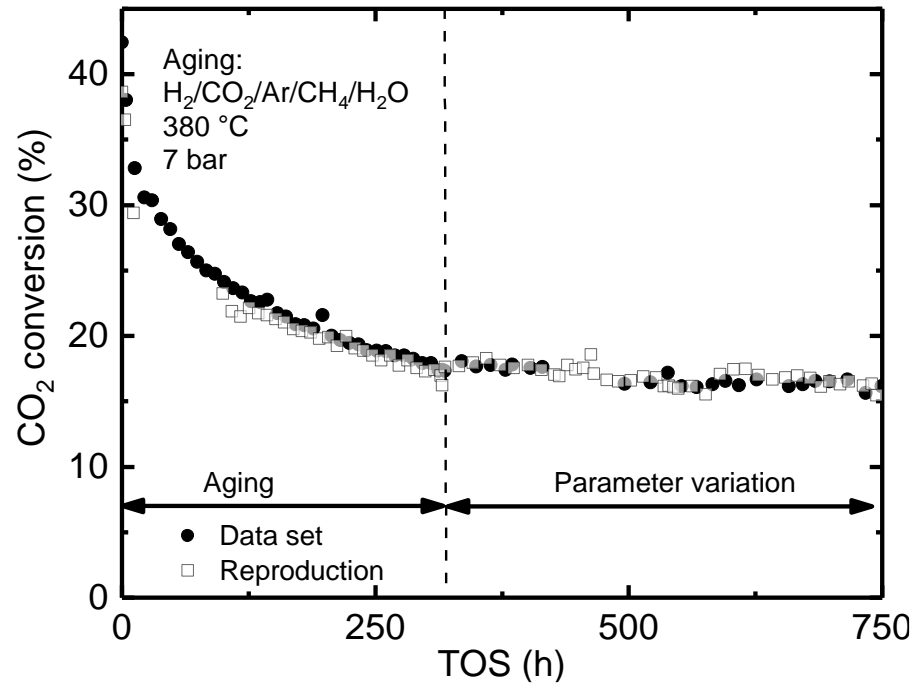
Contactless Temperature Measurements

Spatial resolved temperature measurements:

- Observation of temperature profile and hotspot formation



Kinetic Measurements – Long-term Experiments

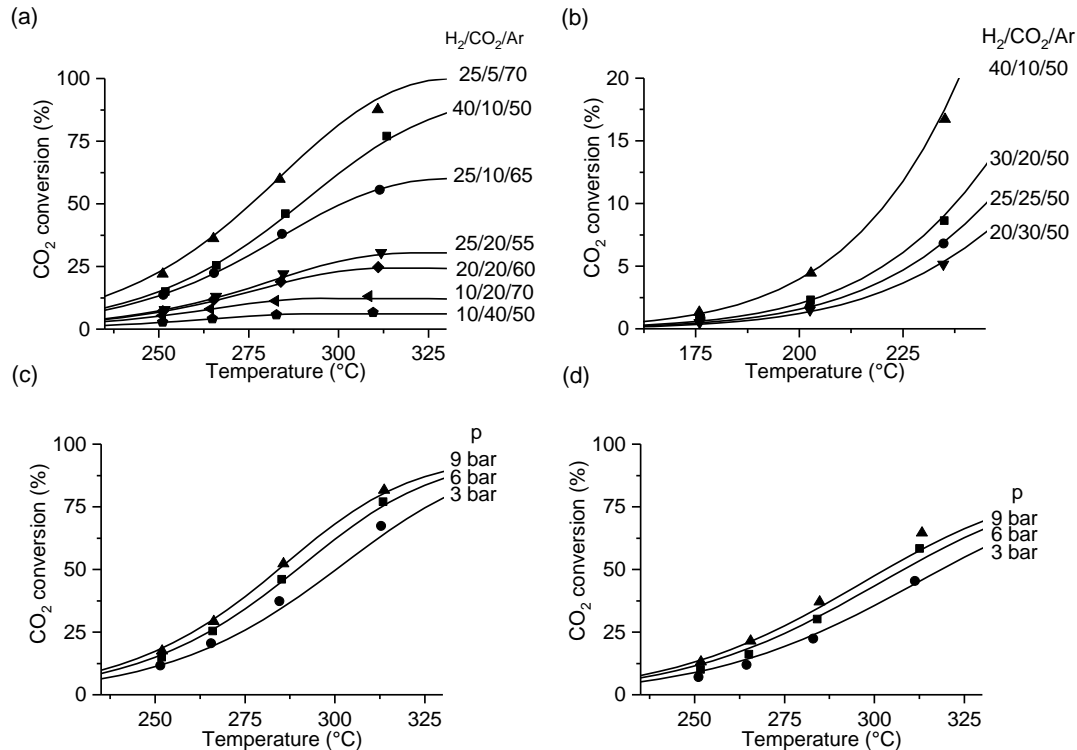


Kinetic data pool

T:	180–340 °C
p:	1–15 bar
H_2/CO_2 :	0.25–8
H_2O/CH_4 :	0/0, 0.25/0.125
m_{cat} :	25 mg, 75 mg

$$r = \frac{k \cdot p_{H_2}^{0.5} p_{CO_2}^{0.5} \left(1 - \frac{p_{CH_4} p_{H_2O}^2}{p_{CO_2} p_{H_2}^4 K_{eq}} \right)}{\left(1 + K_{OH} \frac{p_{H_2O}}{p_{H_2}^{1/2}} + K_{H_2} p_{H_2}^{0.5} + K_{mix} p_{CO_2}^{0.5} \right)^2}$$

Kinetic Measurements – Variation of Reaction Conditions

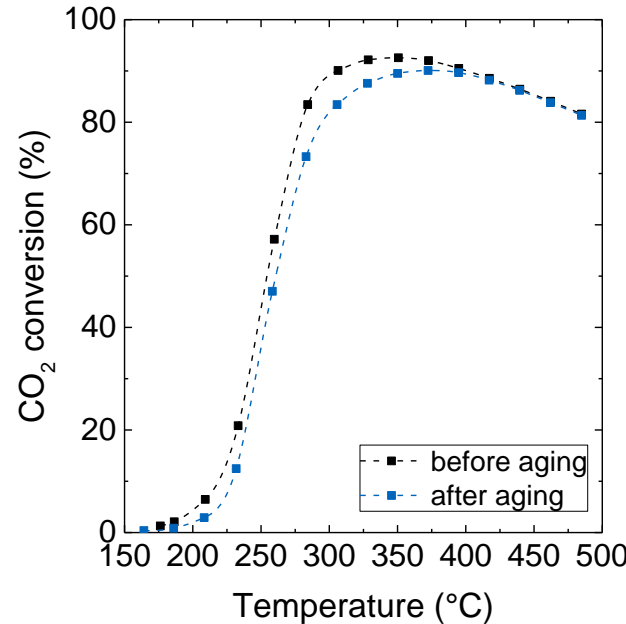
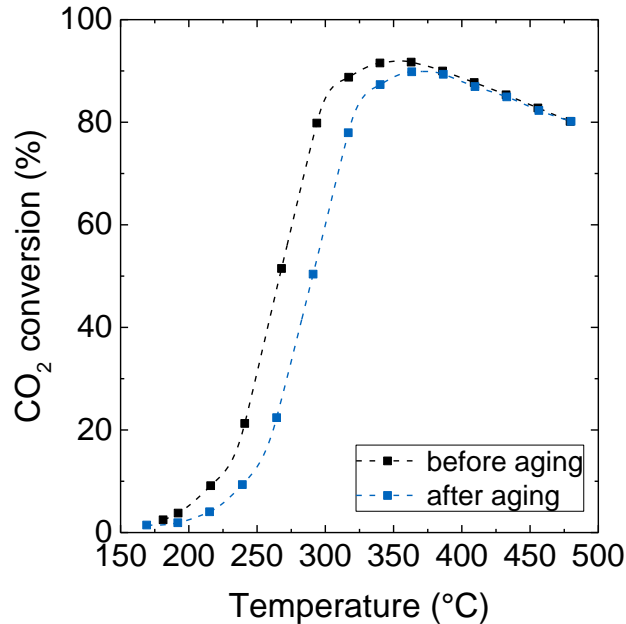


Kinetic data pool

T:	180–340 °C
p:	1–15 bar
H_2/CO_2 :	0.25–8
$\text{H}_2\text{O}/\text{CH}_4$:	0/0, 0.25/0.125
m_{cat} :	25 mg, 75 mg

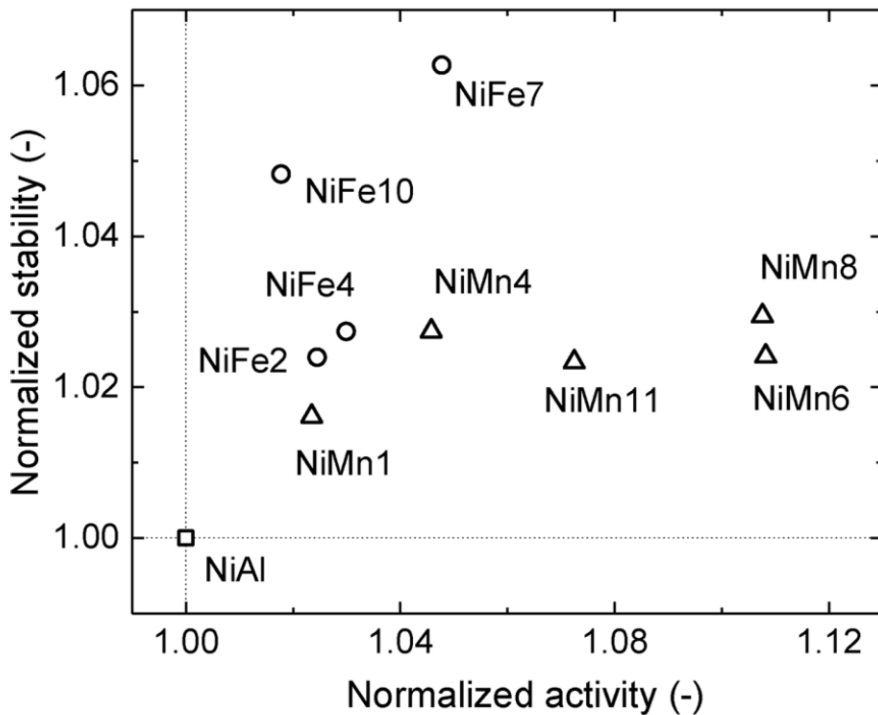
$$r = \frac{k \cdot p_{\text{H}_2}^{0.5} p_{\text{CO}_2}^{0.5} \left(1 - \frac{p_{\text{CH}_4} p_{\text{H}_2\text{O}}^2}{p_{\text{CO}_2} p_{\text{H}_2}^4 K_{eq}} \right)}{\left(1 + K_{OH} \frac{p_{\text{H}_2\text{O}}}{p_{\text{H}_2}^{1/2}} + K_{\text{H}_2} p_{\text{H}_2}^{0.5} + K_{mix} p_{\text{CO}_2}^{0.5} \right)^2}$$

Catalyst Stability



- „rapid aging test“: simulation by aging treatment (500 °C, 32 h, 8 bar)

Catalyst Activity vs. Stability – Influence of Metal Doping

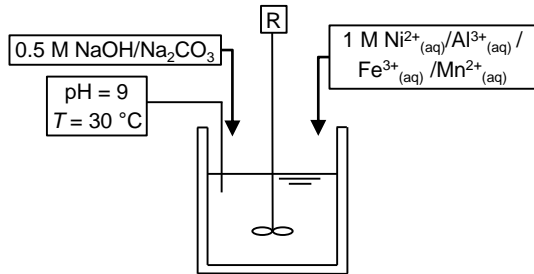


- Highly active and thermostable catalysts can be synthesized
- Synthesis of multimetal-promoted catalysts
 - effects on catalyst activity and stability
 - interactions between promoters
 - alternative synthesis procedures

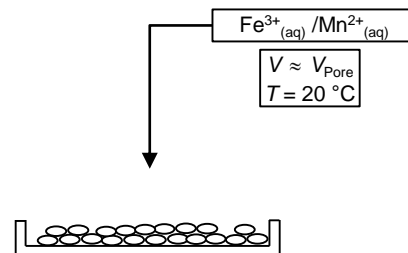
Different Synthesis Strategies for bi-promoted Ni-based Catalysts

Doping of co-precipitated NiAl catalyst *via*...

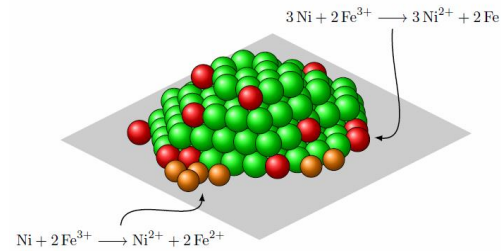
... co-precipitation



... incipient wetness impregnation



...surface redox reaction

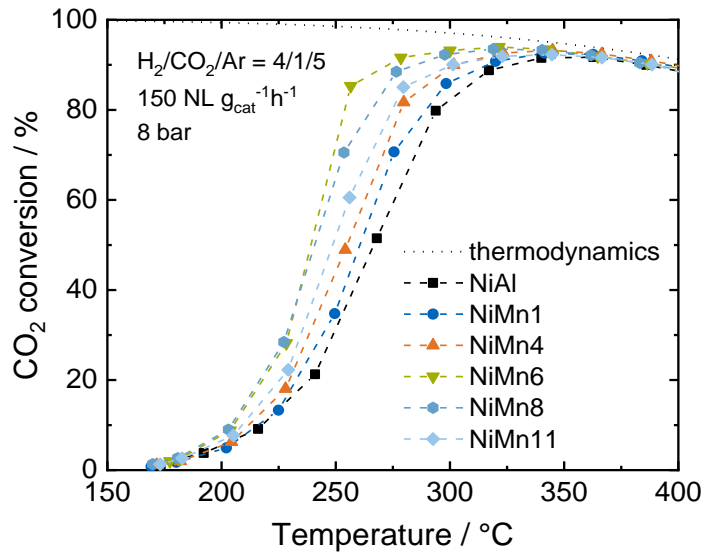


... Ni/Al/Fe/mixed metal oxide

... Fe/Mn deposition on the NiAl mixed metal oxide surface

... Fe and Fe^{2+} deposition on the surface in vicinity to active Ni sites

Dopant Effect of Mn on Co-Precipitated Ni-Al in CO₂ Methanation



Technique	Effect
H ₂ -TPR	reduction signals of Mn ⁴⁺ to Mn ²⁺
XRD	interaction of Mn ²⁺ with mixed metal oxide
IR spectroscopy (CO ₂), CO ₂ chemisorption	increase of basic site density
H ₂ -TPD	identification of Ni sites
CO ₂ -TPD	increase of (esp. medium) basic site density
H ₂ chemisorption	enhancement of Ni particle dispersion



Increase of catalytic activity

Dopant Effect of Fe on Co-Precipitated Ni-Al in CO₂ Methanation

Doping via Co-Precipitation: Fe

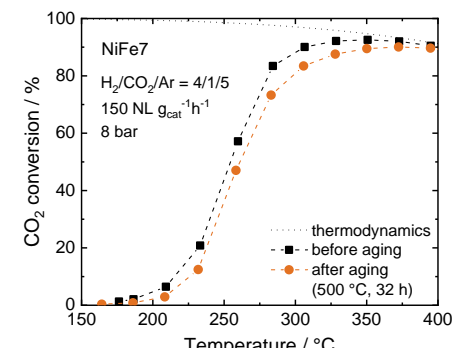
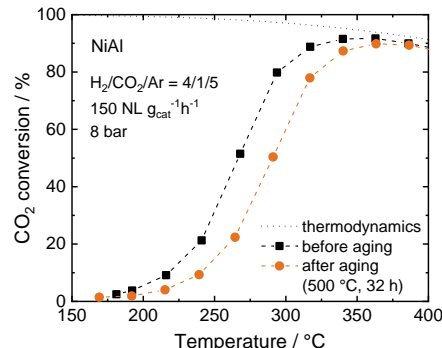
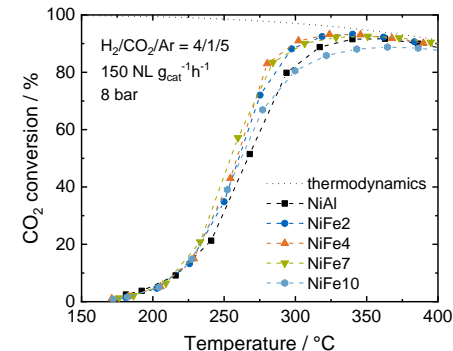
Technique	Effect
H ₂ -TPR	Reduction signals of Fe ³⁺
XRD	Lattice expansion, γFe,Ni formation
FMR	Increase of magnetization, anisotropy
Mössbauer spectroscopy	Formation of γFe,Ni particles
H ₂ chemisorption	Decrease of Ni surface area
H ₂ -TPD	identification of Ni sites
IR spectroscopy (CO ₂ probe)	Change of carbonyl bands



Formation of Ni-Fe alloy particles, electronic modification of the active Ni sites

Increase of

- initial catalytic activity
- apparent thermal stability under CO₂ methanation reaction conditions



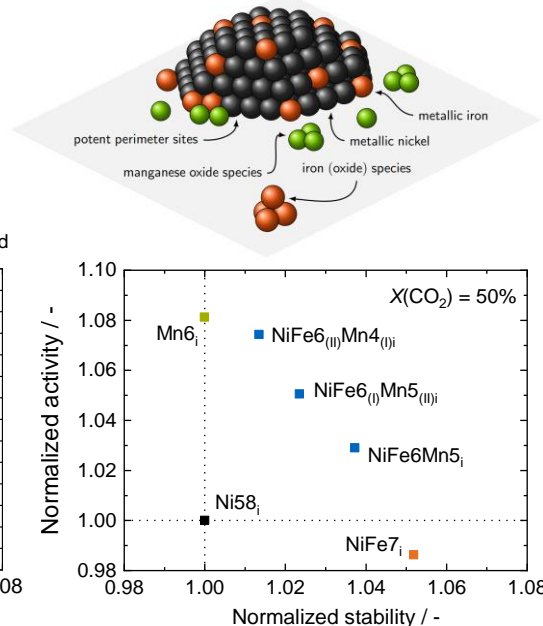
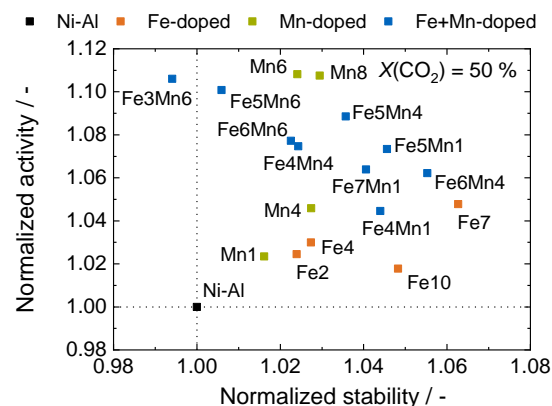
Simultaneous Dopant Effects of Fe and Mn on Co-Precipitated Ni-Al in CO₂ Methanation

Co-Doping of Fe and Mn *via* Co-Precipitation and Impregnation

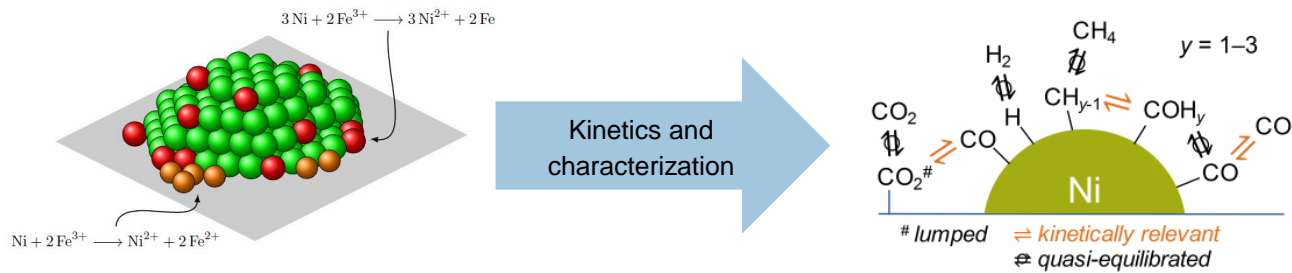
- Improved activity and apparent stability compared to Ni-Al
- Working mechanisms of Fe and Mn similar as in mono-doped catalysts
- Activity-stability behavior of impregnated catalysts depends on doping order and can be tailored



Activity-stability relationship suggests a mechanism involving active perimeter sites



Kinetic Modeling of CO_x Methanation: Reaction Network



Kinetic Modeling of CO_x Methanation: Kinetic Expressions

$$\frac{d\theta_{CO}}{dt} = 0 = r_{ads,CO} - r_{des,CO} + r_{ads,CO_2} - r_{des,CO_2} - r_{Met} + r_{SR} =$$

$$= k_{ads,CO} p_{CO} \theta^* - \frac{k_{ads,CO}}{K_{CO}} \theta_{CO} + k_{ads,CO_2} p_{CO_2} \theta_H \theta^* - \frac{k_{ads,CO_2}}{K_{CO_2}} \theta_{CO} \theta_{OH} - k_{Met} K_{COH_y} \frac{\theta_{CO} \theta_H^y}{\theta^{*y}} \theta^* + \frac{k_{Met}}{K_{Met}} \theta_{CH_{y-1}} \theta_{OH}$$

$$\underbrace{r_{CO}}_{R_{CO}} \quad \underbrace{r_{CO_2}}_{R_{CO_2}} \quad \underbrace{r_{Met}}_{R_{CH_4}}$$

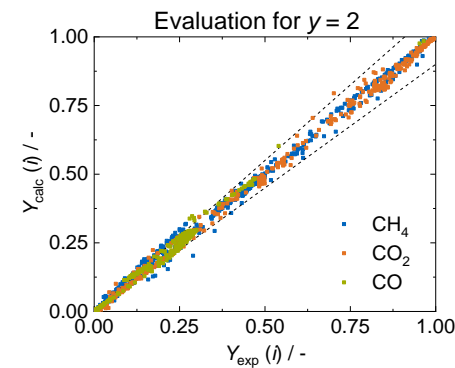
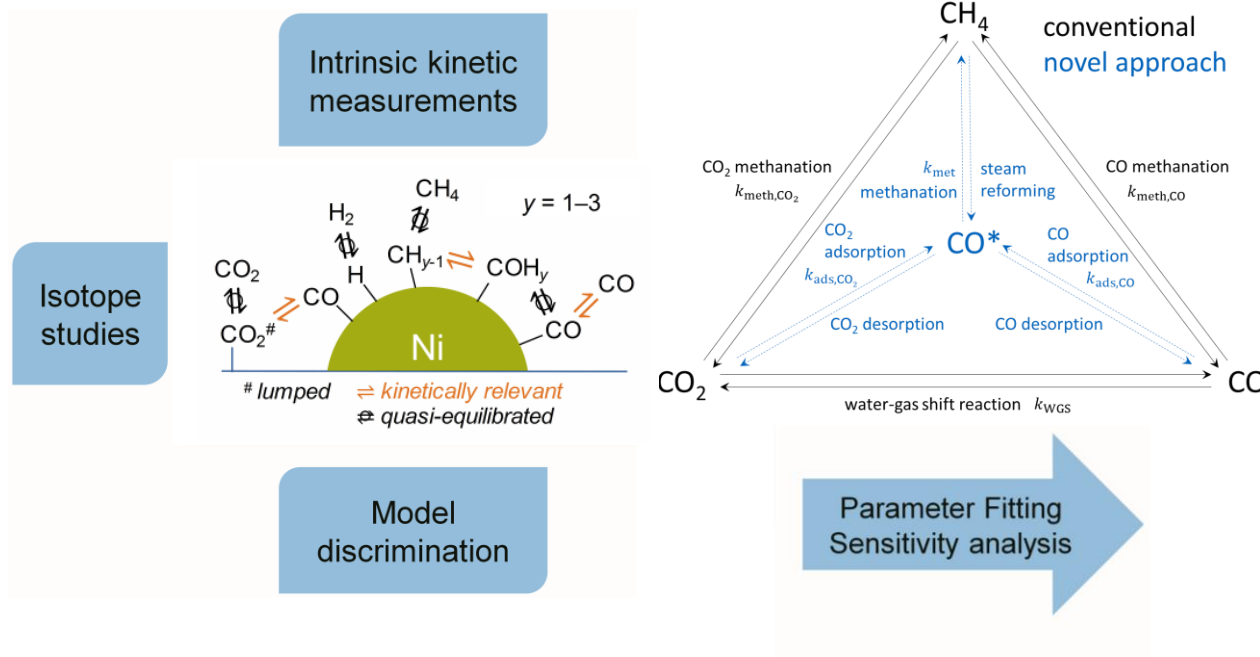
- Methanation reaction mechanism may involve decomposition of different COH_y species
- Minimum sum of squared residuals for a discrete value of $y = 2$
- Kinetic expression for $y = 2$ gives an average on kinetics

Number of parameters: 14
 Number of species: 3
 Number of responses: 1626

Thermodynamic consistency
 Strong Boudart criteria
 Model significance
 Statistic relevance

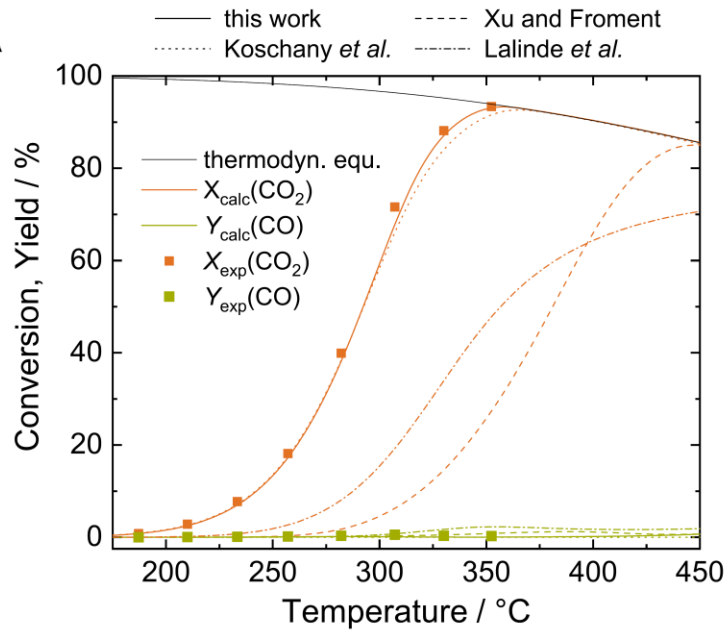
	reparametrized value / -	95 % CI / -
A_{Met} / mol (g _{cat} s) ⁻¹	9.39E+07	-2.58E+07 +3.55E+07
$E_{A, Met}$ / kJ/mol ⁻¹	130.87	±1.41
A_{ads,CO_2} / mol (g _{cat} s) ⁻¹	6.23E+02	-4.80E+02 +6.03E+02
E_{A,ads,CO_2} / kJ mol ⁻¹	56.94	±0.98
$A_{ads,CO}$ / mol (g _{cat} s) ⁻¹	2.35E+03	-1.29E+02 +1.63E+02
$E_{A,ads,CO}$ / kJ mol ⁻¹	56.47	±0.99
$\Delta_{ads}S_{H_2}$ / J (mol K) ⁻¹	-67.51	±1.92
$\Delta_{ads}H_{H_2}$ / kJ mol ⁻¹	-58.38	±1.02
$\Delta_{ads}S_{CH_4}$ / J (mol K) ⁻¹	-217.02	±9.26
$\Delta_{ads}H_{CH_4}$ / kJ mol ⁻¹	-156.45	±5.65
$\Delta_{ads}S_{H_2O}$ / J (mol K) ⁻¹	-135.09	±4.75
$\Delta_{ads}H_{H_2O}$ / kJ mol ⁻¹	-89.85	±2.86
$\Delta_{ads}S_{CO}$ / J (mol K) ⁻¹	-17.56	±1.95
$\Delta_{ads}H_{CO}$ / kJ mol ⁻¹	-44.68	±0.78

Kinetic Modeling of CO_x Methanation: Reaction Network

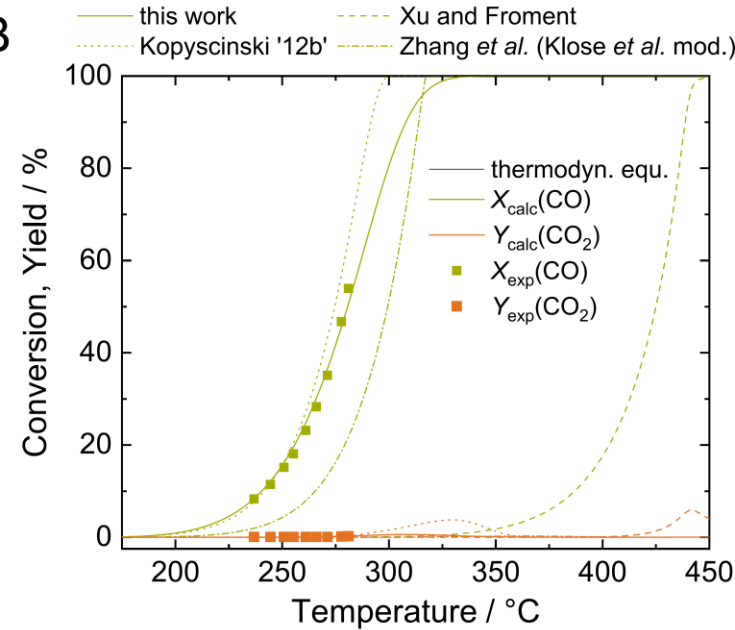


Kinetic Modeling of CO_x Methanation: Results

A



B



Microkinetic Model of CO_x Methanation

- 13 surface species
- 42 elementary steps (forward and reverse reactions)

Available in Chemkin-Format

- This Format is read by catalyticFOAM

The rate coefficient of each reaction is:

$$k_j = A_j T^{\beta_j} \exp\left(\frac{-E_{a,j}}{RT}\right) \exp\left(\frac{\epsilon_{ij} \theta_{ij}}{RT}\right)$$

The production rate of each species is then calculated by:

$$\dot{s}_i = \sum_j \nu_{ji} k_j \prod_i c_i^{\nu_{ji}}$$

Table 2. Detailed, Thermodynamically Consistent Reaction Mechanism for the Methanation of CO and CO₂ over Ni^a

reaction	A_j (cm, mol _s) or S_0 (*)	β_j	$E_{a,j}$ (kJ mol ⁻¹)	ϵ_{ij} (kJ mol ⁻¹)
H ₂ + 2(s) → 2H _(s) (R1)	1.46×10^{-2a}	0	0	
2H _(s) → H ₂ + 2(s) (R2)	4.54×10^{21}	-0.138	96.1	
CH ₄ + (s) → CH ₄ (s) (R3)	1.06×10^{-2a}	0	0	
CH ₄ (s) → CH ₄ + (s) (R4)	2.79×10^{18}	0.085	37.0	
H ₂ O + (s) → H ₂ O _(s) (R5)	1.15×10^{-1a}	0	0	
H ₂ O _(s) → H ₂ O + (s) (R6)	2.04×10^{12}	-0.031	61.0	
CO ₂ + (s) → CO ₂ (s) (R7)	6.29×10^{-9a}	0	0	
CO ₂ (s) → CO ₂ + (s) (R8)	4.99×10^7	0.018	25.8	
CO + (s) → CO _(s) (R9)	3.74×10^{-1a}	0	0	
CO _(s) → CO + (s) (R10)	1.14×10^{12}	-0.103	112.0	50.0^t
CO ₂ (s) + (s) → CO _(s) + O _(s) (R11)	1.60×10^{38}	-1.001	89.3	
CO _(s) + O _(s) → CO ₂ (s) + (s) (R12)	5.81×10^{39}	0	123.6	50.0^t
CO _(s) + (s) → C(s) + O _(s) (R13)	2.36×10^{34}	0	116.2	50.0^t
C(s) + O _(s) → CO _(s) + (s) (R14)	2.54×10^{38}	0	148.1	105.0^t
CO _(s) + H _(s) → C(s) + OH _(s) (R15)	3.05×10^{38}	-0.223	105.3	50.0^t
C(s) + OH _(s) → CO _(s) + H _(s) (R16)	2.18×10^{38}	0.128	62.8	105.0^t
CO _(s) + H _(s) → HCO _(s) + (s) (R17)	6.82×10^{31}	-0.979	132.1	
HCO _(s) + (s) → CO _(s) + H _(s) (R18)	2.18×10^{30}	-0.021	0.2	-50.0^t
HCO _(s) + (s) → CH ₃ (s) + O _(s) (R19)	5.10×10^{35}	0.023	81.7	
CH ₃ (s) + O _(s) → HCO _(s) + (s) (R20)	3.42×10^{39}	-0.023	110.2	
H(s) + C(s) → CH _(s) + (s) (R21)	1.53×10^{34}	-0.456	157.7	105.0^t
CH _(s) + (s) → C(s) + H _(s) (R22)	2.63×10^{32}	0.456	22.3	
CH _(s) + H _(s) → CH ₂ (s) + (s) (R23)	3.21×10^{38}	-0.084	81.1	
CH ₂ (s) + (s) → CH _(s) + H _(s) (R24)	6.16×10^{34}	0.094	95.2	
CH ₂ (s) + H _(s) → CH ₃ (s) + (s) (R25)	7.75×10^{32}	-0.048	59.5	
CH ₃ (s) + (s) → CH ₂ (s) + H _(s) (R26)	6.16×10^{34}	0.048	95.9	
CH ₃ (s) + H _(s) → CH ₄ (s) + (s) (R27)	3.63×10^{32}	-0.048	65.7	
CH ₄ (s) + (s) → CH ₃ (s) + H _(s) (R28)	6.16×10^{32}	0.048	53.6	
H(s) + O _(s) → OH _(s) + (s) (R29)	1.16×10^{34}	-0.176	104.2	
OH _(s) + (s) → H(s) + O _(s) (R30)	7.70×10^{39}	0.176	29.8	
H(s) + OH _(s) → H ₂ O _(s) + (s) (R31)	2.34×10^{30}	0.075	44.1	
H ₂ O _(s) + (s) → OH _(s) + H _(s) (R32)	2.91×10^{21}	-0.075	90.4	
2OH _(s) → H ₂ O _(s) + O _(s) (R33)	1.01×10^{30}	0.251	95.1	
H ₂ O _(s) + (s) → 2OH _(s) (R34)	1.89×10^{38}	-0.251	215.8	
H(s) + CO ₂ (s) → COOH _(s) + (s) (R35)	1.29×10^{35}	-0.46	117.2	
COOH _(s) + (s) → CO _(s) + H _(s) (R36)	1.29×10^{30}	0.46	33.8	
COOH _(s) + (s) → CO _(s) + OH _(s) (R37)	6.03×10^{33}	-0.216	54.4	
CO _(s) + OH _(s) → COOH _(s) + (s) (R38)	1.45×10^{31}	0.216	97.6	50.0^t
COOH _(s) + H _(s) → HCO _(s) + OH _(s) (R39)	4.22×10^{21}	-1.145	104.7	
HCO _(s) + OH _(s) → COOH _(s) + H _(s) (R40)	3.25×10^{39}	0.245	16.1	
2CO _(s) → CO ₂ (s) + C(s) (R41)	6.51×10^{13}	0.5	241.7	100.0^t
C(s) + CO ₂ (s) → 2CO _(s) (R42)	1.88×10^{21}	-0.5	239.3	105.0^t

Microkinetic Model of CO Methanation

- 13 surface sites
- 42 elementary steps

Available in Chem3D
 → This Format is

The rate coefficient

$$k_j = A_j T^{\beta_j} \exp\left(\frac{-E_{a,j}}{RT}\right) e$$

The production ra

$$\dot{s}_i = \sum_j \nu_j k_j \prod_i c_i^{\nu_i}$$

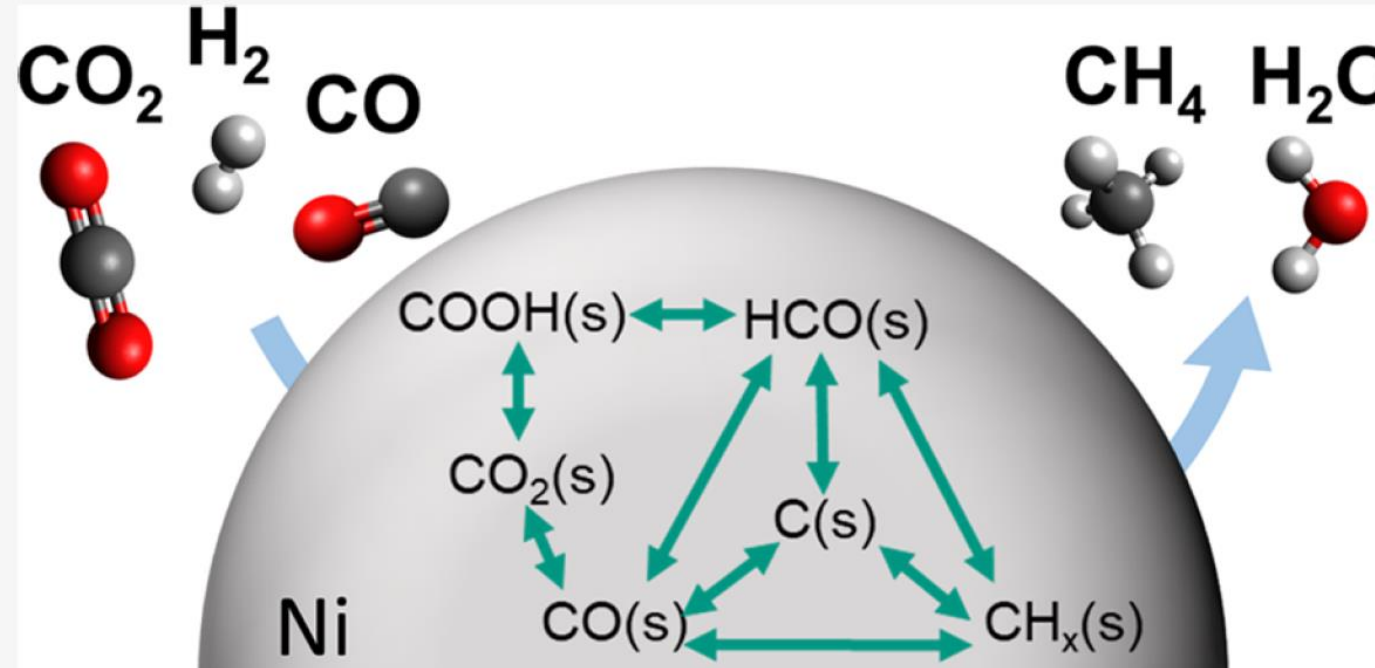
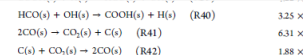


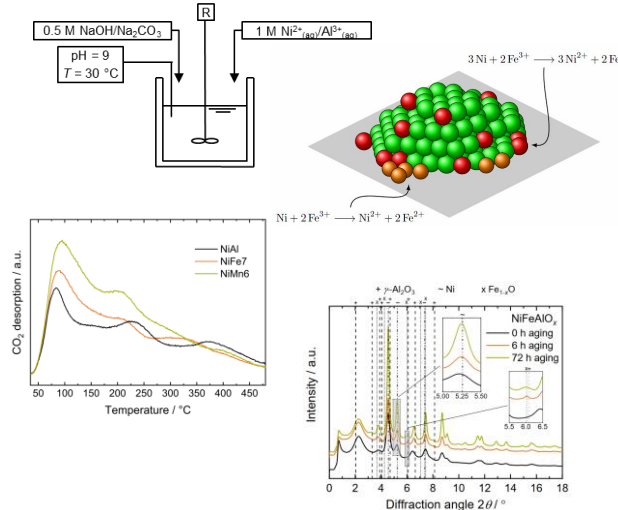
Table 2. Detailed, Thermodynamically Consistent Reaction Mechanism for the Methanation of CO and CO_2 over Ni^a

$E_f (\text{kJ mol}^{-1})$	$\epsilon_f (\text{kJ mol}^{-1})$
0	0
96.1	
0	
37.0	50.0 ^b
0	
61.0	
0	
25.8	
0	
112.0	50.0 ^b
89.3	
123.6	50.0 ^b
116.2	50.0 ^b
148.1	105.0 ^b
105.3	50.0 ^b
62.8	105.0 ^b
132.1	
0.2	-50.0 ^b
81.7	
110.2	
157.7	105.0 ^b
22.3	
81.1	
95.2	
59.5	
95.9	
65.7	
53.6	
104.2	
29.8	
44.1	
90.4	
95.1	
215.8	
117.2	
33.8	
54.4	
97.6	
104.7	50.0 ^b
215.8	
117.2	
33.8	
54.4	
97.6	



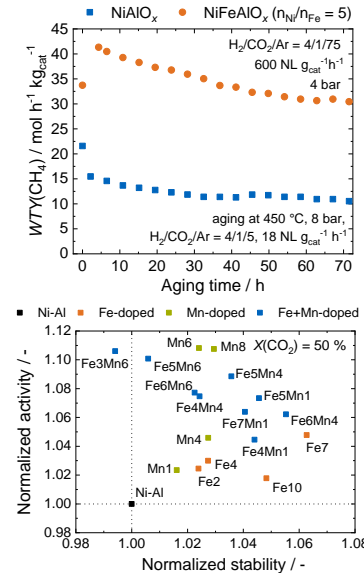
Summary

Catalyst Synthesis and Characterization



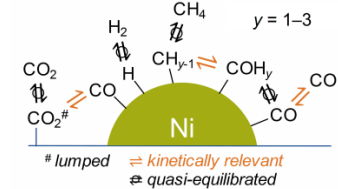
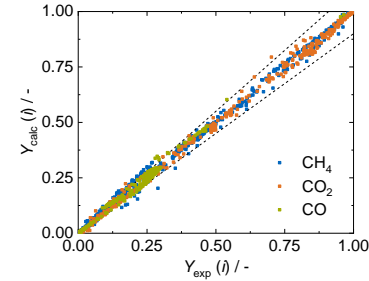
CO₂ Methanation

Structure - Activity Analysis



CO_x Methanation

Kinetic Measurements and Kinetic Modeling



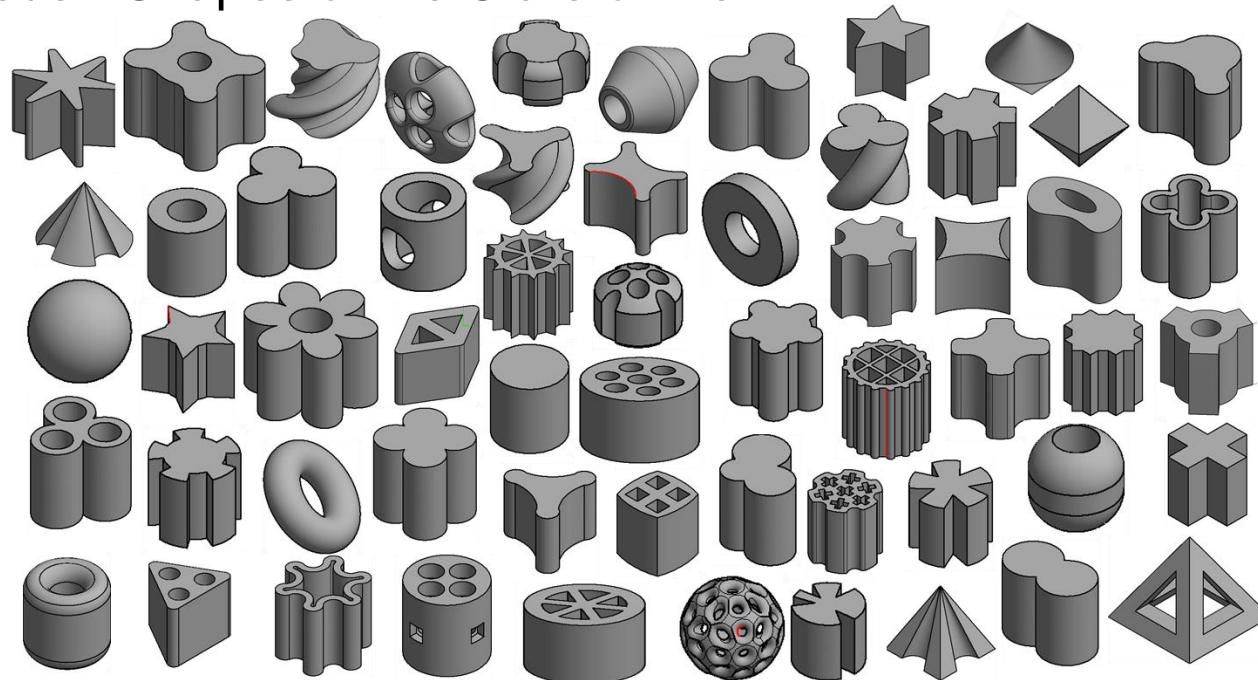
Types of fixed beds

powder bed	random (pellet) bed	structured bed ^[2]	foams ^[1]	periodic open cellular structures (POCS) ^[1]
development – decrease of pressure drop				
+ direct use of catalyst powder - very high pressure drop	+ maintenance + catalyst synthesis + shaping - pressure drop - broad residence time distribution (turbulences)	+ radial dispersion + narrow residence time distribution - wall contact (channeling and heat transport) - sensitive to roundness of tube - adhesion of catalyst	+ even flow profile + high specific surface area - wall contact (channeling and heat transport) - sensitive to roundness of tube - adhesion of catalyst	+ lowest pressure drop + good heat transport + wall contact - low residence time - adhesion of catalyst

[1] A. Inayat et al. Chem. Eng. Sci. 2011, 66, 2758.

[2] A. Gascon et al. Catal. Sci. Technol. 2015, 5, 807.

Pellet Beds - Shapes of the State of the Art?



J. von Seckendorff, PhD Thesis, Technical University of Munich, **2021**.

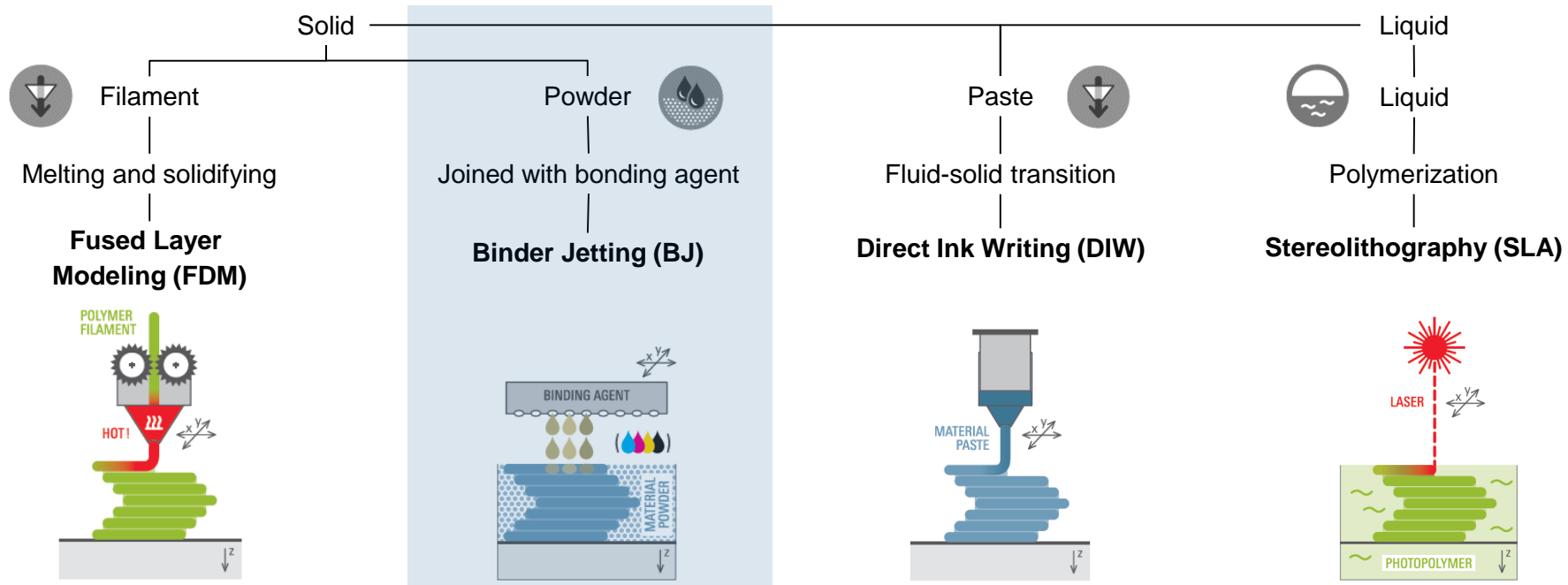
P. Donaubauer, O. Hinrichsen, *IEC Research* **2019**, 58, 110-119.

J. von Seckendorff, P. Scheck, M. Tonigold, R. Fischer, O. Hinrichsen *Chem. Eng. J.* **2021**, 404, 126468. 24

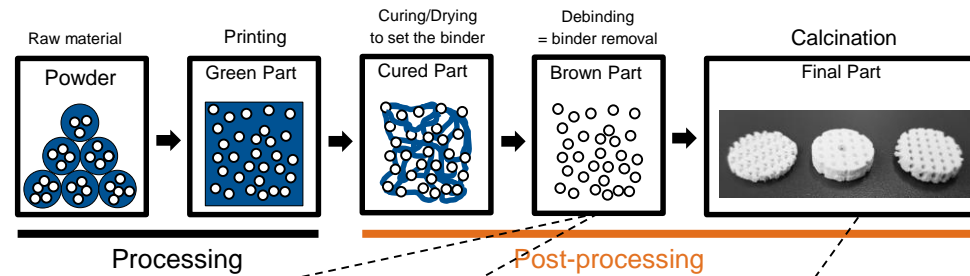
Classification of AM processes for ceramics

For **all** processes: 3D structures are created by a selective layer-by-layer process

Based on DIN 8580 and
Formnext AM Field Guide
Compact (2019)



Binder Jetting (BJ) Fabrication Steps



Shapes still embedded in powder



Removing loose powder



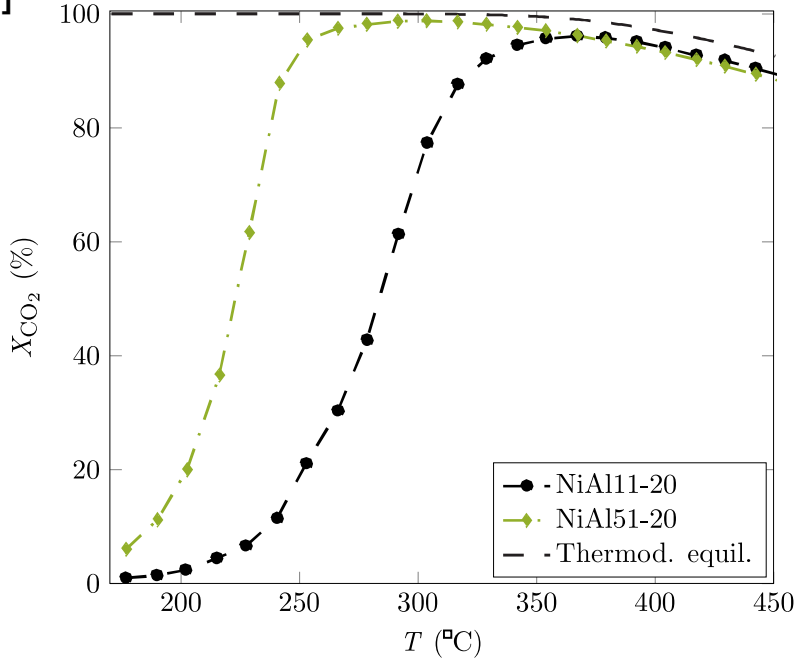
Calcined 3D-printed parts



Reduced catalysts

Preliminary Results for CO₂ Methanation over BJ printed catalysts

[2]



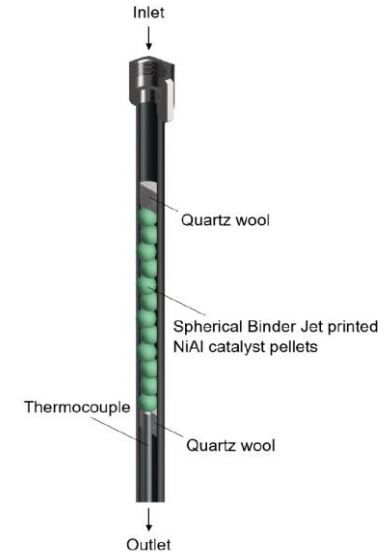
CO₂ methanation

10 cm catalyst packing

p = 9 bar

Feed ratio H₂/CO₂ = 4

[1]



[1] J. Fernengel, L. Bolton, O. Hinrichsen, *CET* **2020**, *43*, 172–178.

[2] confidential results

Ph.D. Students involved

David Schlereth (BASF SE)

Franz Koschany (MAN)

Chris Schüler (Clariant)

Stefan Ewald (Freudenberg)

Philipp Donaubauer (WACKER)

Johanna Fernengel (Clariant)

Moritz Wolf (EPA)

Thomas Burger (Freudenberg)

Tabea Gros

Hanh My Bui

Heike Plendl

Christian Bauer



Bundesministerium
für Bildung
und Forschung



Bayerische
Forschungsstiftung

CLARIANT



Munich Catalysis · MuniCat
Alliance of Clariant and TUM

An aerial photograph of the Technical University of Munich (TUM) campus in Garching bei München. The campus is a large, modern complex of buildings, mostly white with blue roofs, arranged in a grid-like pattern. It is surrounded by green fields, a river to the west, and a road network. In the background, the city of München is visible, along with the majestic Alps under a clear blue sky.

Thank you very much for your attention!

Stay healthy!